

WWJMRD 2017; 3(4): 6-10
www.wwjmr.com
Impact Factor MJIF: 4.25
e-ISSN: 2454-6615

Anjali Maurya
Dr.H.S Gour Central
University, Dept. of
Chemistry, Sagar, India

Nanda Bhatia
B.L.P.Govt.P.G.College
Mhow, Dept. Of Chemistry,
D.A.V.V. Indore (M.P.), India

Microwave assisted chemical synthesis of Tin dioxide

Anjali Maurya, Nanda Bhatia

Abstract

Nanocrystalline SnO₂ has been synthesized by liquid mix technique using citric acid as the complexing agent. The phase, size and purity of the resultant products were characterized by means of powder X-ray diffraction (XRD). Optical studies were carried out by UV-Vis absorption spectroscopy. The morphology and size was confirmed by scanning electron microscopy (SEM) analysis and Transmission electron microscopy (TEM). Presences of functional groups are analyzed by using FTIR spectroscopy.

Keywords: Microwave, Crystalline, Nanoparticles, X Ray Diffraction

Introduction

Tin (Sn) is fiftieth element in the periodic table. It belongs to p-block of the periodic table. These elements are more electronegative and softer than the transition metals. Tin is found in the two different oxidation states 2+ and 4+ in oxide forms known as stannous oxide (SnO) and stannic oxide (SnO₂). Most stable crystal structure of the SnO₂ is rutile with the following lattice parameters $a = 4.373 \text{ \AA}$ and $c = 3.186 \text{ \AA}$, having axial ratio of 1: 0.672. The crystal structure of SnO₂ belongs to the point group of symmetry 4/mm and space group P4₂/mm with Sn and O at 2a and 4f positions respectively. Sn to O ratio is 1:2 in a unit cell which means Sn and oxygen has octahedral co-ordination with 4 O and 2 Sn atoms. Oxygen atoms are surrounded by three Sn atoms, which approximate the corners of an equilateral triangle. It was observed that SnO₂ in [110] surface has no net dipole moment making it non-polar [1]. Tin dioxide (SnO₂), a very important n-type semiconductor with a wide band gap ($E_g = 3.6 \text{ eV}$ at 300 K), is widely used in various areas of electronics [2-3]. Particularly, applications of tin dioxide based ceramics as varistors [4-10] and as humidity sensors [11-13] are known. Varistors are semiconductor devices with nonlinear dependence of current on voltage, which is the same for both voltage polarities [14]. It has been widely used in many applications such as fabricating solar cells, [15-16] electrochemical applications, [17] electrode materials for Li-ion batteries, [18] catalysts for redox reactions, [19-20] and gas sensors. [21-24].

Due to its high sensitivity to reduce as well as to oxidize gases, SnO₂ has been used as the predominant sensing material in the field of solid-state gas sensors for environmental monitoring of CO, H₂, and NO. The large surface area of SnO₂ allows more surface to be available for CO adsorption and the subsequent desorption of CO₂, which in turn would allow for an increase in its sensitivity. [25-26]. Nanosized SnO₂ could enhance the sensor performance because of its microstructural characteristics and electronic properties. It can be found that SnO₂ is one of the most studied materials in all dimensions in the sense of synthesis and fundamental properties evaluations.

Many processes have been developed for the synthesis of SnO₂ nanostructures, e.g., spray pyrolysis [27], hydrothermal methods [28-30], evaporating tin grains in air [31], chemical vapor deposition [32], thermal evaporation of oxide powders [33], rapid oxidation of elemental tin [34], the sol-gel method [35]. In the present work, we report the synthesis of nanostructured SnO₂ by liquid mix technique [36]. The technique is employed to synthesize nanocrystalline SnO₂ at relatively lower temperatures. The method is fast, relatively cost-effective and yields nanopowders with a fairly narrow particle size distribution.

All the above mentioned synthesis techniques were carried out using microwave heating. Microwave heating has such advantages as high-efficiency, rapid-formation nanoparticle, narrow crystallite size distribution and agglomeration diminution with respect to the conventional methods. Synthesis via microwave-assisted routes is simple, energy efficient and time saver. Its utilization results in rapid volumetric heating, high selectivity and great

Correspondence:

Nanda Bhatia
B.L.P.Govt.P.G.College
Mhow, Dept. Of Chemistry,
D.A.V.V. Indore (M.P.), India

product yield with high purity. Energy transfer via microwave irradiation is believed to occur either through resonance or relaxation. Crucial parameters of this method are microwave power, exposure time and energy flow-rate [37-38].

Experimental

All chemicals are analytical grade and are used as received without further purification. Tin dioxide was prepared by taking 16.9g of Tin chloride ($\text{SnCl}_2 \cdot 2\text{H}_2\text{O}$) and 26.25g of citric acid in a glass beaker. Distilled water was added to have homogenous mixture. The solution was evaporated to dryness by exposing it to microwave for 8 minutes. The material turned into a glassy type material. The product obtained was grinded and transferred into a crucible and was kept in a muffle furnace for 30 minutes at a temperature of 400°C , which resulted in the formation of loose off white colored residue. The product obtained (fig 1) was kept for characterization.



Fig 1: Synthesized nanocrystalline Tin dioxide (SnO_2)

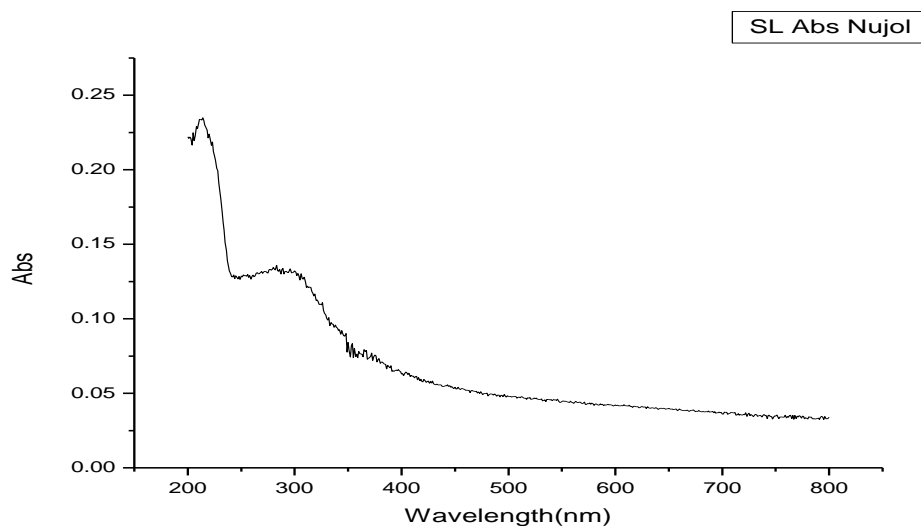


Fig 2: UV VIS spectrum of Tin dioxide

FTIR spectrum of the nanosized tin dioxide powder prepared by microwave assisted liquid mixed technique method is shown in Figure 3. The broad band around $3600\text{--}3201\text{ cm}^{-1}$ region is due to the stretching vibration of O-H bond. This band is due to the OH groups and the adsorbed water bound on the SnO_2 surface [39]. The peak at 1662 cm^{-1}

Characterisation of Nanoparticles

UV-visible absorption spectrum was obtained from Vis-Cary 5E model spectrometer in the wavelength range 200 – 800 nm. FTIR spectra of nickel oxide was recorded in KBr pellets using Shimadzu (model 8400S) spectrophotometer from 4000 cm^{-1} to 400 cm^{-1} . The phase and crystallinity were characterized by using a Bruker D8 Advance Cu $\text{K}\alpha$ radiation ($\lambda = 1.5406\text{ \AA}$, Rigaku Geiger Flex X-ray diffractometer). Surface morphology was studied by JSM-7600F scanning electron microscope. The transmission electron micrographs were taken with a Philips CM-200-Analytical transmission electron microscope working at 120kV.

Results and Discussion

For semiconductor nanoparticles, the quantum confinement effect is expected. Semiconductor nanoparticles with dimensions in the order of the bulk exciton will show unique optical properties, which depend strongly on the size. In semiconductors, band gaps increases with decreasing particle size and the absorption edge will be shifted to a higher energy concomitantly. The absorption spectrum of SnO_2 nanoparticles as prepared is shown in figure 2 the value of the absorption at (220 nm) indicate that the particles are really in the quantum regime. In addition there is a broad absorption band at around 300nm.

is attributed to the bending vibration of water molecules, trapped in the SnO_2 sample. Peaks present in the range from 400 to 1000 cm^{-1} are $478, 617, 638, 748\text{ cm}^{-1}$ due to the presence of different Sn-O and Sn-O-Sn stretching modes [40-42].

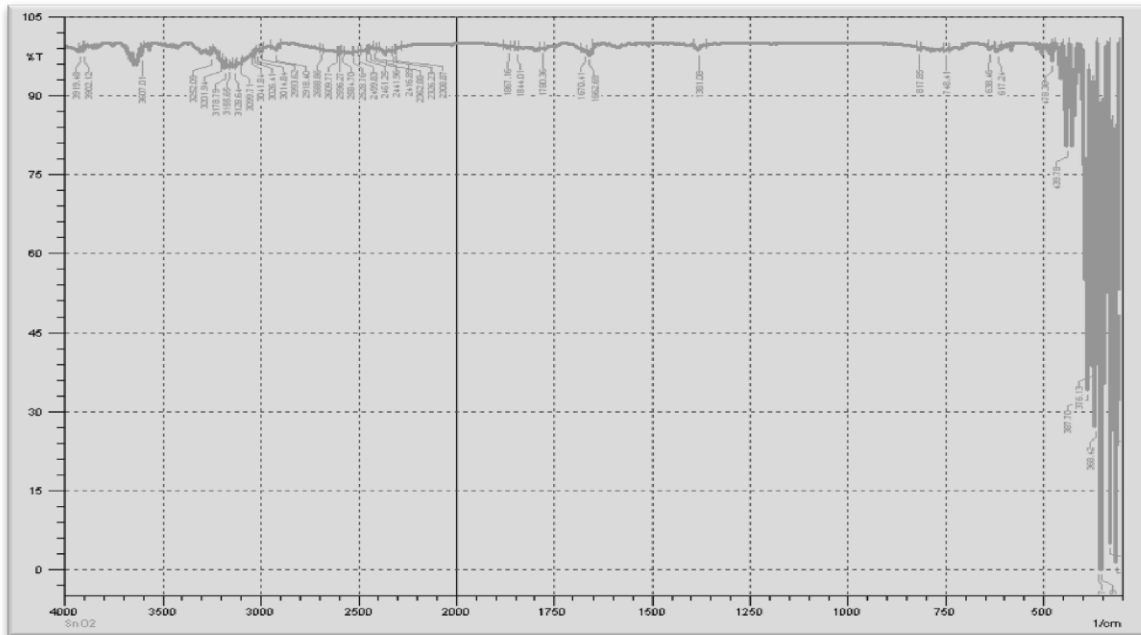


Fig 3: IR spectrum of Tin dioxide

The prepared tin dioxide nanoparticles were examined by powder X-ray diffraction Figure 4 presents XRD pattern of as synthesized SnO₂ nanoparticles. The sample peaks (indexed in the pattern) are well in agreement with JCPDS 41-1445. It reveals a good crystalline tetragonal (p42 mmm) rutile structure with lattice constants a = 4.7355 and c = 3.1879. The peaks at 2θ values of 26.7°, 33.9°, 37.7°,

51.8°, 54.7°, 57.7°, 61.6°, and 64.9°, 65.9°, 71.3°, 78.9°, 83.7° can be associated with (1 1 0), (1 0 1), (2 0 0), (2 1 1), (2 2 0), (0 0 2), (3 1 0), (1 1 2) and (3 0 1), (2 0 2), (3 2 1), (2 2 2) respectively. The crystallite size of the prepared powders calculated from XRD line broadening using Debye Scherrer equation is 25.6 nm.

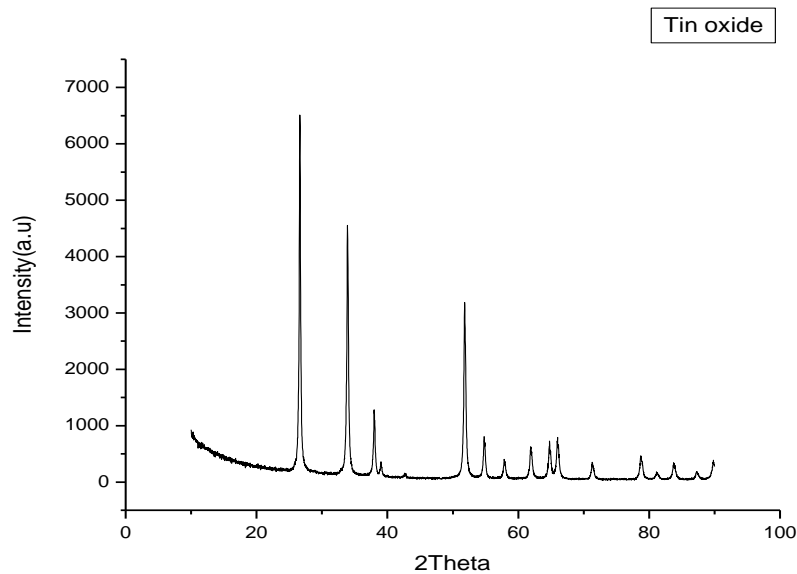


Fig 4: X-ray Diffraction Pattern of Tin dioxide

The scanning electron microscopy (SEM) measurement was carried out in order to analyze the structure and morphology of synthesized material. Figure 5 shows the scanning electron microscopy (SEM) micrograph of the

synthesized SnO₂ sample. Clustering of particles seems to have occurred on the surface. In this image, cubic structures can be easily seen.

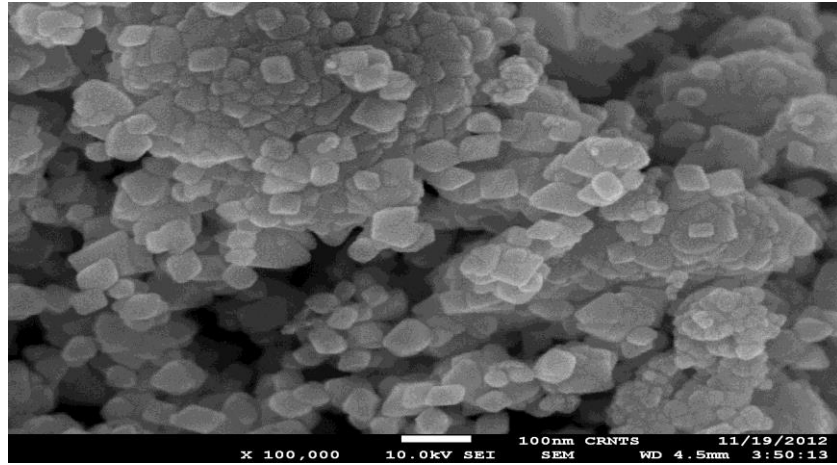


Fig 5: SEM micrograph for Tin dioxide

The TEM micrograph of SnO₂ nanoparticle and its SAED pattern are shown in figure 6A and 6B respectively. It is clear from the figure that the SnO₂ particles are uniform and crystalline in nature. The corresponding ring pattern of SAED confirmed the presence of single crystalline Cassiterite SnO₂ phase nanoparticles. The TEM micrograph allow us to compute the statistical grain sizes

and it reveals the presence of non-agglomerated tin oxide nanoparticle with uniform particle size, which is in the average of about 30.5 nm. This is well matched with the particle size extracted from the XRD measurements. This has also confirmed the presence of single-crystal SnO₂ nanostructure.

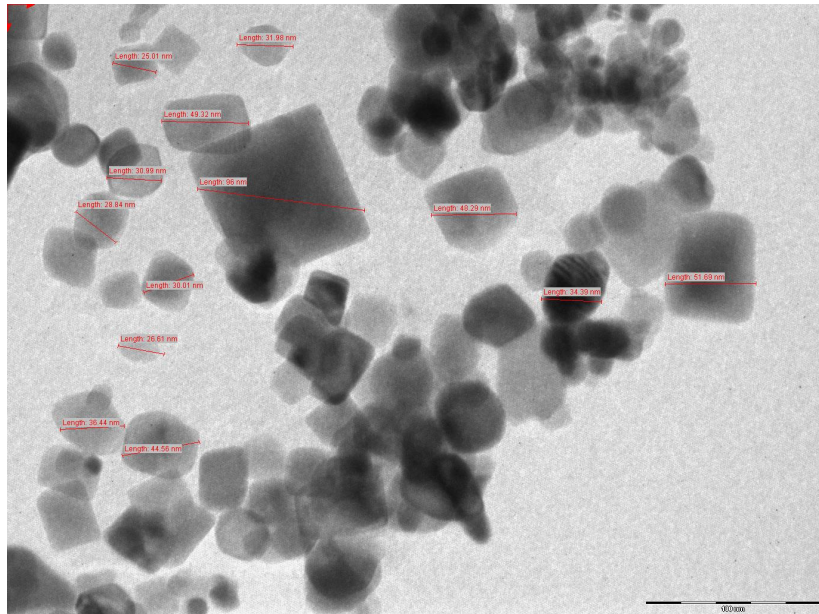


Fig 6: A. TEM Images of Tin dioxide

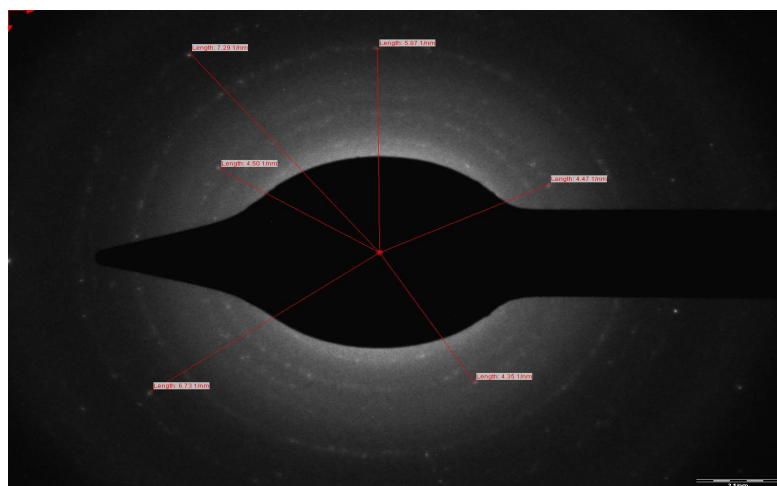


Fig 6: B. TEM (Selected area electron diffraction pattern) of Tin dioxide

Conclusion

Tin dioxide nanoparticles were synthesized by Microwave assisted liquid mix synthesis method using Tin chloride and citric acid as precursors. The UV- VIS spectrum of the synthesized tin oxide nanoparticles sample shows a bands at 220 and 300 nm. FTIR spectrum of the nanosized tin dioxide powder showed Peaks $\sim 478,617,638,748 \text{ cm}^{-1}$ due to the presence of different Sn-O and Sn-O-Sn vibrational modes. The purity and crystallinity of the synthesized SnO₂ nanoparticles examined by powder X-ray diffraction (XRD), revealed a good crystalline tetragonal (p42 mmm) rutile structure, with lattice constants $a = 4.7355 \text{ \AA}$ and $c = 3.1879 \text{ \AA}$. The crystallite size of the prepared powder calculated from XRD line broadening using Debye Scherrer equation is 25.6 nm. The scanning electron microscopy (SEM) measurement was carried out in order to analyze the structure and morphology of synthesized material. Scanning electron microscopy (SEM) micrograph of the synthesized SnO₂ sample shows clustering of particles and, cubic structures can be easily seen. The morphology and sizes of the tin dioxide nanoparticles were analyzed by transmission electron microscopy. The TEM micrograph allow us to compute the statistical grain sizes, revealed the presence of non-agglomerated tin oxide nanoparticle with uniform particle size, which is in the range $\sim 30.5 \text{ nm}$. The corresponding ring pattern of SAED confirmed the presence of single crystalline SnO₂ phase nanoparticles.

References

1. C. Drake, S.Deshpande and S.Seal, *Appl. Phys. Lett.* 89 (2006) 116.
2. M.S. Gudiksen, L.J. Lauhon, J. Wang, D. Smith, C.M. Lieber, *Nature* 415 (2002) 617.
3. W.U. Huynh, J.J. Dittmer, A.P. Alivisatos, *Science* 295 (2002) 2425.
4. A. B. Glot, A. M. Chakk, B. K. Chernyi and A. Ya. Yakunin, *Inorganic Materials*, 10 (1974) 1868.
5. A. Ya. Yakunin, B. K. Chernyi, A. M. Chakk and A. B. Glot, *Inorganic Materials*, 12 (1976) 803.
6. A.B. Glot, 20 (1984) 1522.
7. A. B. Glot and A. P. Zlobin, *Inorganic Materials*, 25 (2) (1989) 274.
8. A. B. Glot, N. Yu. Proshkin and A. M. Nadzhafzade, *Ceramics Today Elsevier*, 66 (1991) 2171.
9. P. N. Santhosh, H. S. Potdar and S. K. Date, *J. Mat. Res.*, 12 (1997) 326.
10. S. A. Pianaro, P. R. Bueno, E. Longo and J. A. Varela, *Ceramics International*, 25 (1999) 1.
11. A.B. Glot, "The Conduction of SnO₂ Based Ceramics", *Inorganic Materials*, 20 (10) (1984) 1522
12. B. M. Kulwicki, *Am. Ceram. Soc.*, 74 (1991) 697.
13. E. Traversa, "Ceramic Sensors for Humidity Detection: the State-of-the-art and Future Developments", *Sens. Actuators B*, 23 (1995) 135.
14. G. D. Mahan, L.M. Levinson and H.R. Philipp, *J. Appl. Phys.*, 50 (1979) 2799.
15. T.W Kim, D. U Lee, D. C Choo, J. H Kim, H Kim, J Jeong, J. H. Jung, M. Bahang, J. H.Park, H. L Yoon, Y. S. Kim, *J. Phys. Chem. Solids* 63(2002) 881.
16. T. E Moustafid, H Cachet, B Tribollet, D Festy., *Electrochim. Acta.* 47(2002)1209.
17. M Okuya, S Kaneko, K Hiroshima, I Yaggi, K Murakami., *J. Eur. Ceram. Soc.* 21 (2001) 2099.
18. C Kim, M Noh, M Choi, Cho, J Park, B. *Chem. Mater.* 17 (2005) 3297.
19. L Chou, Y Cai, B Zhang, J. Niu, S Ji, S Li., *Appl. Catal. A Gen.* 238 (2003)185.
20. P. T Wierzychowski, L. W Zatorski., *Appl. Catal. B Environ.* 44 (2003) 53.
21. A. J Moulson, J. M Herbert, *Electroceramics*, Chapman & Hall, New York, (1990).
22. Y Shimizu, M Egashira., *MRS Bull* 24.(1999) 18.
23. H. C Wang, Y Li, M. J. Yang, *Sens. Actuators. B Chem.* 119 (2006) 380.
24. G. J Li, X. H Zhang, S Kawi., *Sens. Actuators. B Chem.* 60(1999) 64.
25. Pei et al. *Materials Research.* 13(2010) 339.
26. Abdul Rahim Yacob, Mohd Khairul Asyraf Amat Mustajab, and Nur Syazeila Samadi World Academy of Science, Engineering and Technology 56 (2009).
27. F. Paraguay-Delgado, W Antúnez-Flores, M Miki-Yoshida, A Aguilar-Elguezabal, P Santiago, R Diaz, J.A Ascencio,*Nanotechnology* 16 (2005) 688.
28. B Cheng, J.M Russell, W Shi, L Zhang. E.T Samulski, *J. Am. Chem. Soc.* 126, (2004) 5972.
29. F. Du, Z Guo, G Li, *Mater. Lett.* 59 (2005) 2563
30. S Fujihara, T Maeda, H Ohgi, E Hosono, H Imai, S Kim., *Langmuir* 20 (2004) 6476.
31. J Duan., S Yang, H Liu, J Gong, H Huang, X Zhao, R Zhang, Y. J Du., *Am. Chem. Soc.* 127 (2005) 6180.
32. Y.Liu, E Koep, M Liu., *Chem Mater* 17 (2005)3997.
33. Z.R Dai, J.L Gole, J.D Stout, Z.L Wang, *J. Phys. Chem. B* 106 (2002)1274.
34. J.Q Hu, X.L Ma, N.G Shang, Z.Y Xie, N.B Wong,C.S Lee, S.T Lee, *J. Phys. Chem. B* 106, (2002) 3823
35. F. Pourfayaz, A Khodadadi, Y Mortazavi, S.S Mohajerzadeh, *Sensors Actuators B* 108 (2005) 172.
36. M.P. Pechini, U.S. Patent, 3,330,697 (1967).
37. T. Krishnakumar, R. Jayaprakash, N. Pinna, V.N. Singh, B.R. Mehta and A.R. Phani, *Materials Letters*, 63(2) (2009) 242.
38. Mirosław Zawadzki, *J. Allo. Com.*451 (1-2), (2008) 297.
39. Zhang, G.; Liu, M. *J. Mater. Sci.* 34(1999) 3213
40. Acarbas, O.; Suvaci, E.; Dog_n, A. *Ceram. Int.*, 33 (2007) 537.
41. A. Die'guez, A. Romano-Rodriguez, J. R. Morante, U. Weimar, M.Schweizer-Berberich, and W. Go'pel, *Sens. Actuators. B.* 31(1996) 1.
42. J.F. Scott, *J. Chem. Phys.* 53 (1970) 852.